C. R. Physique 16 (2015) 26–36

Contents lists available at ScienceDirect

Comptes Rendus Physique

www.sciencedirect.com

Granular physics / Physique des milieux granulaires

Strain localisation in granular media

Localisation de la déformation dans les milieux granulaires

Jacques Desrues [b,a,*], Edward Andò [b,a]

[a] *Université Grenoble Alpes, 3SR, 38000 Grenoble, France*
[b] *CNRS, 3SR, 38000 Grenoble, France*

ARTICLE INFO

Article history:
Available online 21 February 2015

Keywords:
Strain localisation
Granular materials
Triaxial and biaxial tests
X-ray tomography
Full-field measurements
Precursors of localisation

Mots-clés :
Localisation de la déformation
Matériaux granulaires
Essais biaxiaux et triaxiaux
Tomographie à rayons X
Mesures de champs
Précurseurs de localisation

ABSTRACT

This paper discusses strain localisation in granular media by presenting experimental, full-field analysis of mechanical tests on sand, both at a *continuum* level, as well as at the *grain scale*. At the continuum level, the development of structures of localised strain can be studied. Even at this scale, the characteristic size of the phenomena observed is in the order of a few grains. In the second part of this paper, therefore, the development of shear bands within specimen of different sands is studied at the level of the individual grains, measuring grains kinematics with x-ray tomography. The link between grain angularity and grain rotation within shear bands is shown, allowing a grain-scale explanation of the difference in macroscopic residual stresses for materials with different grain shapes. Finally, rarely described precursors of localisation, emerging well before the stress peak are observed and commented.

RÉSUMÉ

Cet article est une introduction à la physique de la localisation de la déformation dans les milieux granulaires. Il présente les caractéristiques essentielles du phénomène d'émergence et de développement de structures de déformation localisée, qu'on appelle généralement des bandes de cisaillement. Il s'appuie sur l'observation expérimentale de champs de déformation dans des essais mécaniques de laboratoire, à deux échelles d'observation : l'une, macroscopique, à laquelle le milieu granulaire est observé comme un milieu continu, et l'autre, qu'on qualifiera de microscopique sans notion d'unités de mesure, à l'échelle du grain. À l'échelle macroscopique, l'observation continue quantitative par des techniques photogrammétriques révèle l'apparition du phénomène et son développement sous forme de structures à l'échelle de l'échantillon. Même à cette échelle, la taille caractéristique des phénomènes observés se révèle être de quelques grains. À l'échelle microscopique, un suivi exhaustif en 3D de tous les grains d'échantillon de sables soumis au même type d'essais peut désormais être réalisé en utilisant la microtomographie à rayons X, et c'est l'objet de la seconde partie de cet article. Le lien entre l'angularité des grains et leur rotation dans les bandes est montré, ce qui permet d'avancer des explication microscopiques à diverses observations macroscopiques qui ignorent l'aspect discret du milieu. Incidemment,

* Corresponding author.
E-mail address: jacques.desrues@3sr-grenoble.fr (J. Desrues).

http://dx.doi.org/10.1016/j.crhy.2015.01.001
1631-0705/

des phénomènes rarement décrits – qui paraissent être des précurseurs de localisation apparaissant bien avant le pic – sont observés et commentés.

1. Introduction

Strain localisation in granular media is both a commonplace and fascinating phenomenon. Indeed, it is common experience that dykes, levees, trench walls, and other man-made as well as natural soil structures most often show so-called "failure surfaces" at rupture, rather than overall plastic deformation; on the other hand, the sudden emergence of a shear band in a carefully prepared homogeneous laboratory specimen loaded with well-controlled boundary conditions that do not introduce measurable symmetry breakage or heterogeneity seed, is a wonder for the experimentalist trying to catch the mysteries of strain localisation. It is much less a wonder for his engineering colleagues, who perform such tests to characterise the stress–strain response of the material, and usually rely on elasto-plastic constitutive equations to model it as a continuum medium and apply numerical methods, *e.g.*, Finite Element Method, in order to design structures: they need constitutive data, measured with reasonably good repeatability on supposedly homogeneous specimens. Strain localisation does not enter easily into the mould of constitutive modelling and numerical simulations: it contradicts the basic assumptions of homogeneous and unique response of the specimens, and it requires significant mathematical refinements in the theoretical and numerical frameworks in order to be accounted for rigorously and efficiently.

This issue of strain localisation in granular media in the context of continuum mechanics has been studied by different researchers around the world, both experimentally and theoretically, since the beginning of the 1970s [1–11]. The present article, being in the context of a set of papers devoted to "granular physics", will try to bridge the gap between this long-standing and intensive quest and the more recent emergence of grain-scale approaches to the behaviour of granular media. In fact, it appears that none of the two perspectives can be simply disregarded: strain localisation belongs essentially to both the structural scale, let us call it macroscale, and the material scale, which is in essence a matter of microstructural evolution, *i.e.*, grains in the case of granular media. Hence, the paper will be organised in two parts, one presenting a brief synthesis of the macroscale or continuum observations of strain localisation, and the second dealing with the new results on the microstructural aspects of strain localisation, that become increasingly accessible to observation thanks to the formidable progresses of imaging techniques in the last 10 years.

2. Macroscopic observation of strain localisation

Strain localisation in soils has been recognised implicitly as the essential issue regarding natural and man-made geotechnical structures' stability for centuries by engineers. Coulomb's paper on a theoretical approach of soils mass stability [12] is probably the most famous "foundation" text of soil mechanics, introducing the concept of internal friction in bulk granular media. Indeed, this paper relies on the hypothesis of a sliding rigid block over a (rectilinear) rupture surface to analyse this situation: here we find strain localisation. However, the essence of the link between the small strain response of granular media as a continuum, and the occurrence of strain localisation, has started to be the object of intensive experimental and theoretical studies only since the 1970s, parallel with the development of constitutive and numerical modelling for granular media.

2.1. Methods for analysis of strain localisation in the continuum framework

The methods used to experimentally explore the onset and development of strain localisation in granular media, like in other solids essentially resort to image analysis. More precisely, speaking of the development of a deformation process over a domain, a differential approach based on a comparison of successive images of a deforming object is required. False Relief Stereophotogrammetry (FRS – used on such images in the 1980s and 1990s [13,14][1]), followed by digital image correlation have allowed the precise quantification of the strain field in sand and rock specimens subjected to plane strain tests. The increasing resolution of the acquired images, as well as the performance of image correlation are still allowing new measurements to be made today, especially on the multiscale aspects of localisation. Simultaneously, computerised tomography (CT) has allowed the non-destructive imaging not only of the surface of specimens, but throughout their volume as well. With the increasing resolution of CT scanners, Digital Image Correlation (sometimes referred to as DVC – since 3D images are sometimes called "volumes") has become applicable in 3D since the middle of the 2000s. It is possible today to accurately characterise the complex 3D strain fields that develop in bulk specimens subjected to non-homogeneous mechanical tests performed in situ, *i.e.*, directly in the x-ray beam. This was initially done using powerful x-ray sources

[1] The False Relief Stereophotogrammetry technique relies on a human operator based, quantitative interpretation of the false vertical relief obtained when observing a pair of successive 2D images of a plane object. The *false* relief is interpreted as a displacement field. This operation is performed on a suitable machine (stereocomparator) such as the one used for topographic measurements.

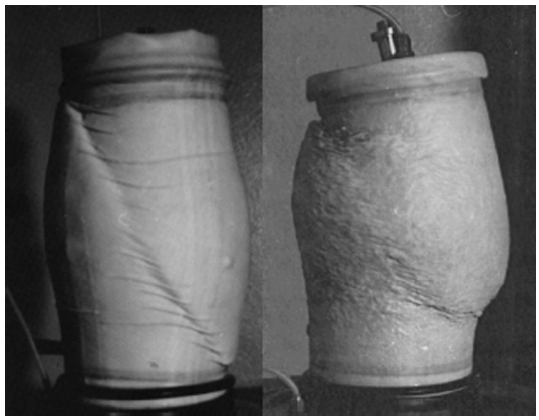

Fig. 1. Shear bands observed in triaxial specimens on fine and coarse sand, left and right respectively.

(synchrotrons) available in large installations like ESRF in Grenoble, then on laboratory x-ray scanners such as the one the authors have been operating in Laboratoire 3SR, Grenoble, France, since 2008. The most recent evolution in this constantly progressing experimental quest has been the development of the discrete 3D approach of deforming sand specimens using microtomography.

2.2. Continuum observations of strain localisation

Strain localisation in granular media essentially belongs to both the macroscopic and the microscopic scale. Fig. 1 illustrates these two aspects: it shows two 100 mm diameter sand specimens (enclosed within a flexible membrane) subjected to axisymmetric triaxial loading in compression, which consists of progressively shortening in the axial direction while the entire specimen is subjected to an isotropic confining pressure applied by a fluid. The essential difference between these two tests is the mean grain size: 0.32 and 3.2 mm. It is clear that the shear band emerging in these two tests affects the whole specimen, which does not behave as a representative homogeneous volume but rather as a structure, as soon as localisation starts. On the other hand the shear band thickness is significantly affected by the grain size, as can be seen in the figure. The photos shown are taken with the pressure cell removed at the end of the test, and therefore represent the only observation of the localisation process that can be made for this kind of classical test. Because of this limitation with classical tests, a comprehensive study of the onset of localisation has been undertaken with a specially designed biaxial cell, which allows photos to be taken *during* a test, and therefore allowing incremental strain field to be characterised.

So-called biaxial tests have been used extensively to study strain localisation [2–7,10]. Like the triaxial test, the biaxial test consists in shortening a pressured-confined specimen (always inside a flexible membrane), with the important difference that the specimen, which is a parallelepiped in this case, is constrained to zero deformation (plane strain) in one of the two lateral directions. Hence, the strain field observable on the corresponding face is representative of the strain field through the specimen. High-resolution photographs can be taken along the test, and analysed using image correlation methods evoked briefly above: false relief stereophotogrammetry (FRS) and digital image correlation (DIC).

Fig. 2 shows the following kinematic fields: incremental displacement V, deviatoric strain ϵ_s and volumetric strain ϵ_v measured between eight strain increments in a biaxial test on a specimen of sand, whose stress/strain curve is shown in Fig. 3, on which the different states that have been imaged are numbered. The strain fields presented show that localisation of strain starts before the peak in the specimen's stress response, in increment 3–4. When strain localisation initiates, two parallel shear bands are born (see the measurements of ϵ_s), which indicates that the possible singularity presented by the corner of the specimen is not an essential determining factor in the initiation of the band, and that the orientation is a strong characteristic property of the phenomenon.

The strain fields also bear witness to the fact that the pattern of localised strain may change as the test continues, to finally result in a kinematically admissible mechanism (*i.e.*, compatible with the boundary conditions), unlike the mechanism first seen in increment 3–4.

Furthermore, the strain fields also reveal that volumetric strain (in the form of increase/decrease in volume: dilatancy/contractancy), accompanies the deviatoric loading. This is particularly the case at the beginning of strain localisation (what follows thereafter in the shear band corresponds essentially to noise).

A synthesis of the studies of strain localisation in sand carried out with stereophotogrammetry in Laboratoire 3SR (previously "IMG") in Grenoble has been published in [10] and [7].

In parallel with the biaxial test campaigns developed in Grenoble and several other places (Germany, Japan, USA), computed tomography was used by the first author and doctoral students on axisymmetric triaxial tests on Hostun sand in early works performed at the beginning of the 90s [15,16]. These studies, not detailed here, brought important results on the self-organisation of strain localisation patterns in axisymmetric bodies, where the emergence of shear bands needs some

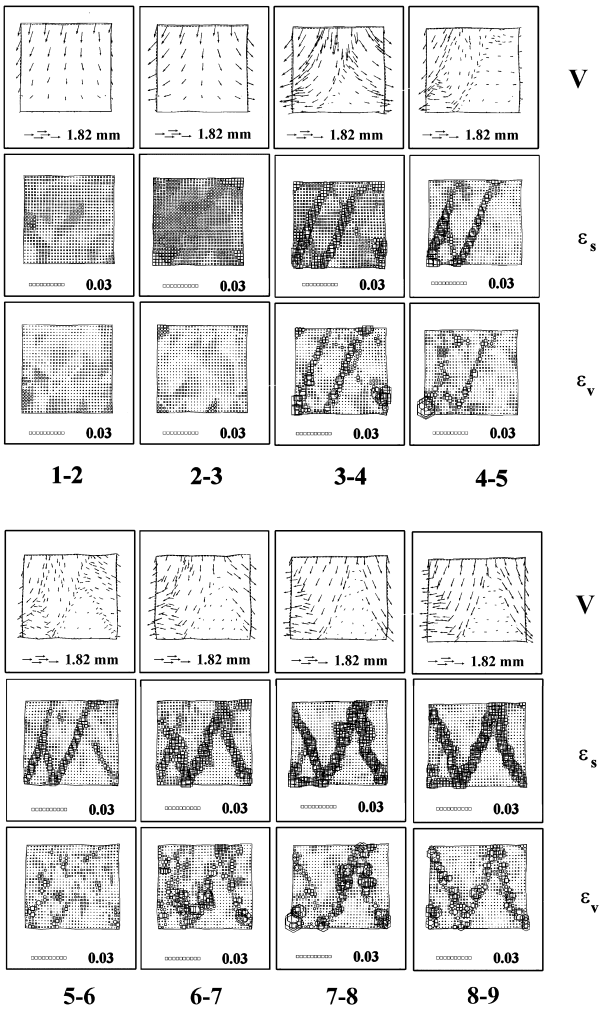

Fig. 2. Characterisation of strain localisation in a biaxial test on sand using stereophotogrammetry from [10].

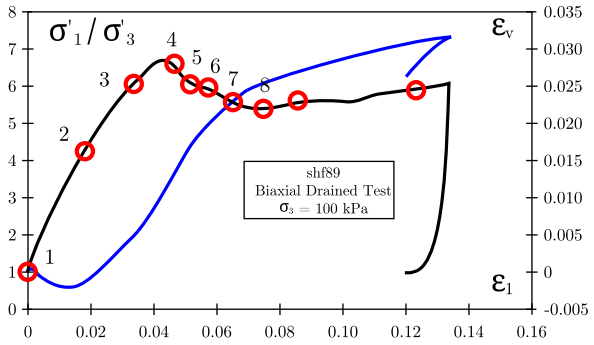

Fig. 3. (Color online.) Stress–strain response of specimen *shf89*. In black the stress ratio (σ_1/σ_3) against axial strain (ϵ_1). In blue the volumetric strain response (ϵ_v) against axial strain.

symmetry breaking to take place; and also, last but not least, the rapid evolution of the void ratio towards a plateau whose the value can be identified as the true critical void ratio for the specific mean pressure at which the test is run.

As for an analysis of the physical causes of strain localisation, the tests performed during the 1980s and 1990s have validated the concept of a self-catalytic process resulting from the development of a local damage or degradation of the material in every point of the specimen, tending to concentrate in kinematically admissible deformation modes that concentrates the damage in narrow bands of material. The focus was put on the first evident damage process in dense sands, namely dilatancy, which can be seen as a kind of internal constraint that requires a dense granular assembly to dilate in

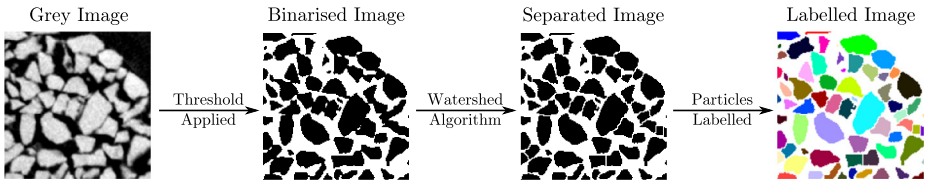

Fig. 4. (Color online.) Very simplified illustration of the grain-identification procedure used.

order to shear. However, dilatancy is not the only possible damage process in granular media: other microstructural features affecting the fabric of the material, such as changes in grain contact distribution, both in number and orientation, attrition that erodes the grains under deformation, grain breakage and crushing at higher mean pressures, are candidates in the list of localisation-promoting processes and can give rise to shear bands in non-dilating granular assemblies like loose sands [Figure 13 in 17], and even compaction bands in which uniaxial compaction occurs at an orientation perpendicular to σ_1, see [18,19].

These observations at the level of the macroscopic specimens lead to the formulation of hypotheses concerning the detailed evolution of the microstructure, that can be better assessed by exploring directly the localisation of deformation at the grain scale. This has become possible only recently, and it is the subject of the second part of this paper.

3. Microscopic observation of strain localisation

3.1. Methods

As introduced in the previous section, during strain localisation in a granular medium (for example during the formation of a shear band) the material's *microstructure* manifests itself strongly during the material's response (governing, for example, the width of the shear band). In order to understand such phenomena more profoundly, they must be observed directly at the relevant microscale. In the case of coarse-grained granular media such as the sand discussed above, the relevant microscale is the *grain scale*.

Previous efforts to obtain direct experimental access to this scale has lead to developments such as $1\gamma 2\epsilon$ in Grenoble, which allows stresses or strains to be applied on a wall made of an analogue 2D "Schneebeli" material composed of thousands of rods whose front face can be photographed, allowing them to be individually identified while they rearrange [20,21]. A recent review of particle-level measurements, including force chains in photoelastic disks can be found in [22].

X-ray tomography has been widely used to explore the 3D deformation behaviour of geomaterials such as sand, since the 1990s [16]. Advances in x-ray technology in the last decade have meant that the spatial resolution has increased to the point where *each sand grain* in a small specimen can be imaged. Due to the inherently non-destructive nature of x-ray tomography, (and in the same style as the photographs in the previous section) specimens can be deformed using specially designed, x-ray transparent equipment, and re-imaged after some deformation has taken place.

Each 3D image (measuring approximately $1500 \times 1500 \times 1500$ voxels – 3D "volume" pixels) can then be analysed individually, using relatively standard image analysis tools in order to binarise (see Fig. 4) the image into two phases: solids and voids. Further processing using a 3D watershed algorithm allows the solid phase to be split into individual grains with relatively high fidelity; these split grains can then be labelled individually. Once labelled, these digital grains can be measured using standard image analysis tools – their position (centre-of-mass) with respect to the origin of the 3D image can be calculated with very good sub-voxel precision (in the images presented here, the D_{50} is around 300 µm, the pixel size 15.56 µm/px and the error on the position of the grains 0.05 pixels in each direction, or 0.003 D_{50}), and a voxelised 3D volume can also be obtained.

Since there is no guarantee that the same grain will have the same label in two images, recent work has developed an algorithm (ID-Track [23]) to recognise grains between different labelled images, using invariant grain properties such as their volume. With this "grain tracking" procedure, the displacement of a grain is easily defined by following its centre-of-mass. Local strains can be obtained from a cloud of grain positions and displacements, which can be tessellated in 3D to yield tetrahedra on which the full strain tensor is defined. The accurate measurement of 3D rotations requires grain-based image correlation [see: 24], which proves more reliable than following the change in orientation of the long and short axes of the grains, since they are not uniquely defined.

The process of splitting the grain phase into individual grains inherently introduces the notion of grain-to-grain contacts: if two grains are split by the watershed algorithm, then they must have been in contact (to within a function of the spatial resolution of the image). Contacts are the points at which force is transmitted through a granular medium, and their evolution (existence, orientation, size) with time is key for understanding phenomena at the grain scale. Since the choice has been made to image a large and therefore *mechanically representative* number of grains, grain-to-grain contacts are imaged with insufficient resolution to overcome orientation biasses in the watershed algorithm. Recent work ([25]) presents an algorithm to overcome these biasses. Furthermore, when the solid phase is identified using a threshold which gives a globally correct volume of solids, our current work shows that the number of contacts is *systematically* overestimated due to the partial volume effect of two bodies at the contact.

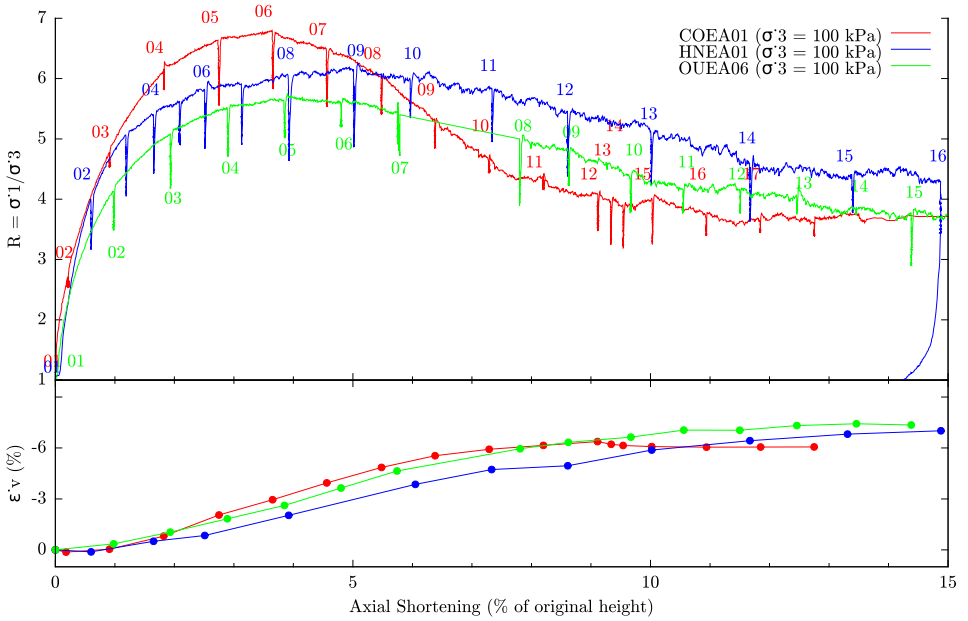

Fig. 5. (Color online.) Triaxial test responses for three tests on Caicos Ooids (COEA01), Ottawa sand (OUEA06) and Hostun sand (HNEA01), performed at a cell pressure of $\sigma_3 = 100$ kPa. The volumetric strain (ϵ_v) response of each material is dilatant.

3.2. Observations

An experimental campaign of dense, small-scale triaxial compression tests was carried out in a specially designed x-ray transparent cell on specimens of sand within the Laboratoire 3SR x-ray scanner, varying sand grain shape and confining pressure for the tests. The specimen size has been fixed to 11-mm diameter and approximately 22-mm height (much smaller than standard) so that specimens can be scanned entirely by a conical x-ray beam at a level of magnification such that *each grain* of the approximately 50,000 in each specimen can be individually identified in each image, with the procedures described above. In these small-scale tests, failure occurs with shear banding, as is expected with these dense materials and indeed as it does in full-scale triaxial tests.

The three materials tested are, in order of increasing roundness, Hostun HN31 sand ($D_{50} = 338$ μm), Ottawa 50/70 sand ($D_{50} = 310$ μm) and Caicos ooids ($D_{50} = 420$ μm). The first two materials are quartz sands, Caicos ooids are an oolitic sand from the Ambergris Shoal in the Caicos platform (Turks and Caicos Islands) in the British West Indies. The grains are composed of calcium carbonate (>96% aragonite), and instead of being the result of an erosion, they grow from an initial seed, which gives them their roundness. The analysis presented focuses on a campaign of 13 triaxial compression tests performed on these materials prepared in a relatively dense (around 90% of relative density) arrangement by dry pluviation and tested at two different confining pressures (100 and 300 kPa).

Fig. 5 shows the stress/strain responses for the three granular materials mentioned above, all tested at 100 kPa confinement pressure. As expected for dense granular media, the overall volumetric response is dilatant, and there is a well-defined peak in the axial stress response of each specimen, followed by a stress-plateau (*n.b.*, that it is possible to explore the post-peak behaviour since the experiment is performed under strain control). Please note that the stress relaxations which are numbered are the points during the test at which loading has been interrupted in order to scan the specimen at a zero strain rate.

Taking COEA01 as an example, Figs. 7 and 8 present vertical cross sections, oriented in such a way to contain both the axis of the specimen and the normal to shear band that eventually forms. In Fig. 7, on the top row, grains are coloured by their *coordination number* (number of grains in contact) in a given state, and in the bottom row are presented local fields of porosity calculated from the binarised images, with a measurement window approximately equal to the size of a grain.

In Fig. 8 grains are coloured by incremental quantities coming from grain tracking, such as their vertical displacement (top row) or the magnitude of their 3D rotation (bottom row) over a given increment. The middle row shows strain measurements (described above) derived from grain displacements. Obviously all the scalars shown are defined and measured in 3D for almost all the approximately 54,000 grains in this specimen.

The coordination number maps show that the grains in the specimen have quite a range of coordination numbers, which is simply explained by the fact that this material is not *mono-disperse*, and therefore the larger grains will naturally tend to have more contacts than the smaller ones. The evolution of this quantity throughout the test shows that a band of grains with reduced coordination numbers develops, indications of which can be seen clearly in state COEA01-07, and perhaps as

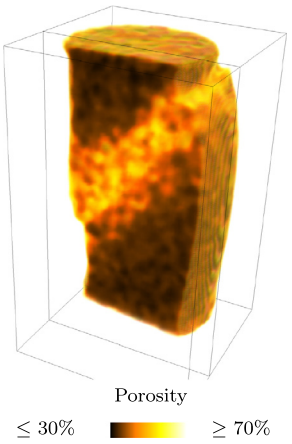

Fig. 6. (Color online.) 3D rendering of the porosity field of state COEA01-17.

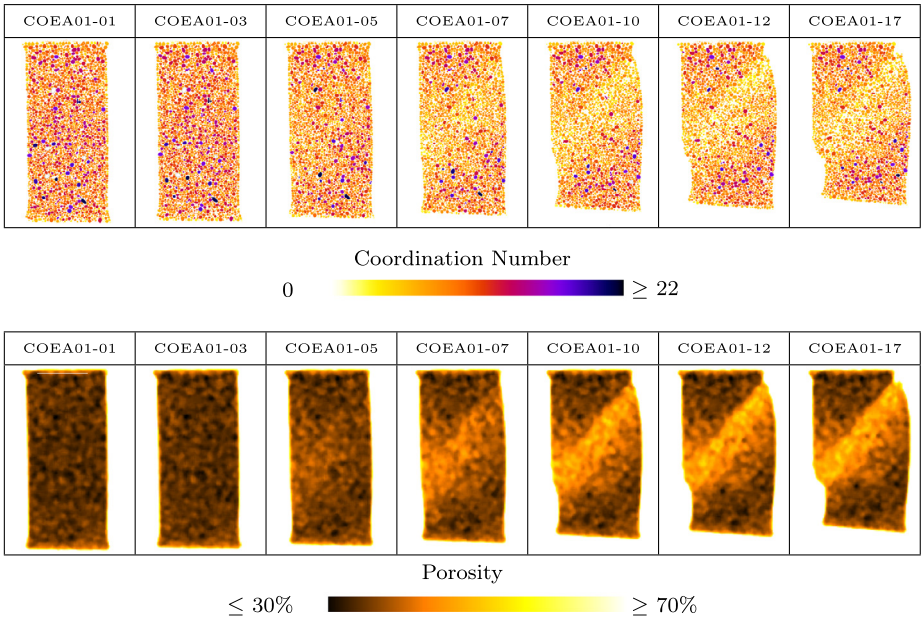

Fig. 7. (Color online.) Slices from some selected states in the test COEA01. In the top row, each grain is coloured by its coordination number; in the bottom row field of local porosity measurements.

early as COEA01-05 (just before the peak). This band of reduced-number-of-contacts (*i.e.*, less dense material) corresponds well to the *dilatant shear band* that is clearly visible in Fig. 6, and in the bottom row of Fig. 7.

The rich kinematic measurements presented in Fig. 8 tell a clear story: at the beginning of the test there is a smoothly increasing displacement field (top row), which corresponds to a homogeneous deformation field (middle row), with very small grain rotations (bottom row) – a good indication that the specimen is well-prepared and that the initial axial compression results in a uniform response. Soon afterwards, however, symmetry is lost, and already the next increment shows a tilting of the vertical displacement field, with a correspondingly concentrated strain in the top right of the section. In the following increment (COEA01-03-04) concentrated rotations also start to appear, and these well before the peak in the axial stress response. The complex and wide patterns of co-rotating grains that are visible in the increments leading up to the peak (COEA01-04-05 and -05-06) are organised into a wide band that traverses the specimen, which can also be seen in the strain field. Further shearing after the peak causes grain rotations and deviatoric strain to concentrate into a tight band.

A remarkable feature of the incremental deviatoric strain maps in Fig. 8 is the occurrence of a network of tiny shear bands, starting from increment COEA01-03-04 (*i.e.*, well before the peak – COEA01-06), which appear to operate at a scale larger than the grain, but smaller than the shear band which emerges as the final failure mechanism at the scale of the specimen. This confirms recent observations of early strain localisation events in rocks [26], evolving internal structures of deformation in an analogue 2D material [27] and glass beads in biaxial compression [28].

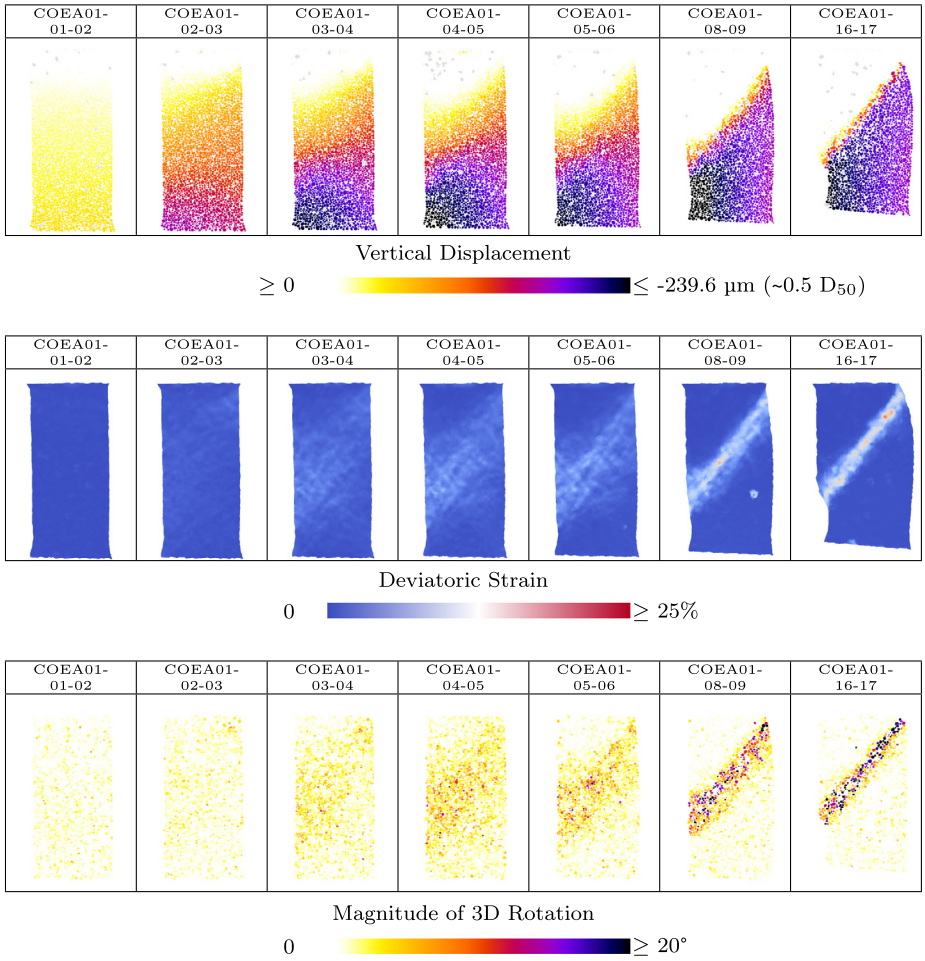

Fig. 8. (Color online.) Slices from some selected increments in the test COEA01. In top and bottom rows, each grain is coloured by a scalar quantity (vertical displacement (negative = upwards) or magnitude of 3D rotation over an increment) with untracked grains are shown in light grey. In the middle row a field if deviatoric strain is shown.

Comparing now the results of the tests on the three materials whose responses are shown in Fig. 5, for each of them Fig. 9 shows grain rotations and deviatoric strain maps measured on an increment in the residual stress state. The deviatoric strain can be seen to be strongly localised in a thin band for all specimens. In HNEA01-15-16, discrete zones of very intense shear (in red) can clearly be seen inside a band which is wider than that in COEA01-16-17 and which has a less abrupt transition in shear strain intensity bordering the band. This is best viewed by looking at the extent of the values of zero deviatoric strain in these specimens. Furthermore, the most intensely shearing zones in HNEA01-15-16 are towards the lower side of the band on the left of the slice, and are towards the upper side of the band on the right side of the slice. No such deviation is present in COEA01-16-17, where the intensely shearing blocks are in the middle of a tight band.

The deviatoric strain in OUEA06-14-15 is localised into a band of variable thickness: in the slice shown, the right side of the band is thicker than the left side, which is tightly concentrated. The change in the shear strain intensity at the border of this band is not as sharp as COEA01-16-17, but sharper than HNEA01-15-16.

The fields of rotations in the bottom row of Fig. 9 show a very concentrated band of grains with intense rotations aligned with the band of high shear strain in all three cases. Counting the numbers of grains with intense rotations across the band reveals that six to eight grains have considerably higher rotations than the rest of the specimen in each case. The values of rotations for this band of grains is very large for COEA01, with many grains rotating more than 20°. The values of rotations for both OUEA06 and HNEA01 in their residual stress increments are 10–15°, but it is important to stress that the increment HNEA01-15-16 is much larger than the other two; normalising by the size of the increment, rotations would be in the order of 5–8°. The intensity of rotations in these three specimens therefore appears to be inversely correlated with grain angularity. In all three specimens, however, there is clearly a band of intensely rotating grains.

In the most angular material (that is to say in increment HNEA01-15-16), a layer of grains with smaller, but non-zero rotations is visible all along the band on both sides of it. The same effect is visible to a smaller extent in OUEA06, with one or two grains on either side of the band. In COEA01, in many places along the edges of the band there appears to

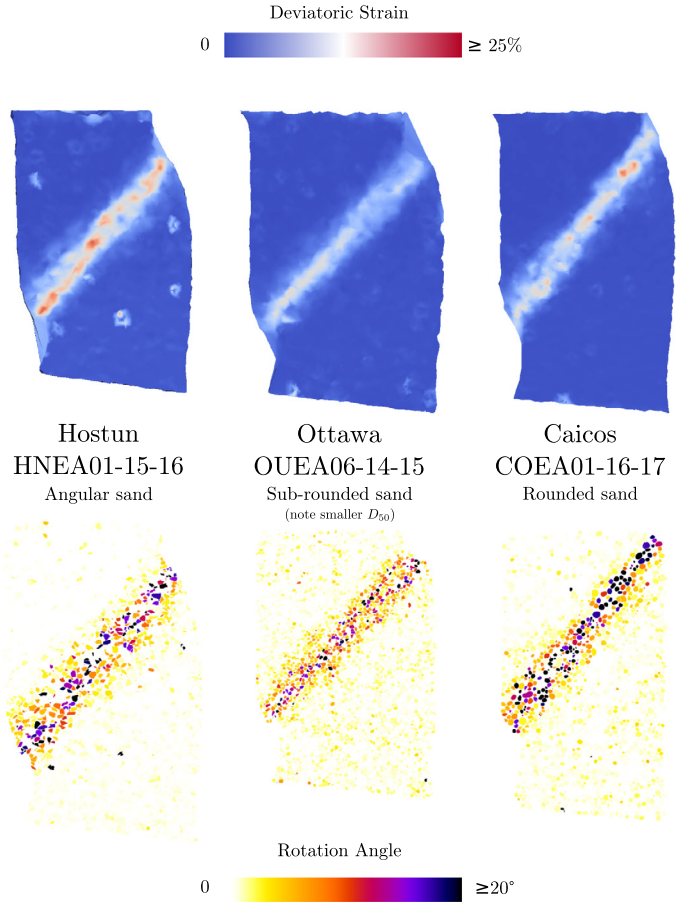

Fig. 9. (Color online.) Deviatoric strain and grain rotations in the final increments of COEA01, OUEA06, HNEA01, adapted from [29].

be no layer of grains with smaller, but non-zero values of rotation; several grains with over 20° rotation can be seen to be touching grains with close to zero rotation. These smaller, but non-zero rotations seem to be correlated with grain angularity, which seems logical because of the interlocking between the particles: the most angular particles are the least free to rotate without causing other particles to rotate simultaneously.

In the residual stress states of these three specimens different micromechanisms are at play: in the rounded material, there is intense grain rotation in thin band of grains, whereas in the angular material there is a band of grains with less intense rotation that is more widely distributed. In Caicos and Ottawa specimens, when the shear band develops, grain shapes offer little resistance to rotation (and therefore to shear), which is why the band is so concentrated. In the angular material however, the fact that grains are not able to rotate as freely as in the other materials means that larger resistance to shearing is obtained. Although shearing is localised in the specimen, for further shear to occur, grains bounding the shear band also need to rotate (due to grain geometries), which limits the rotations and dissipates energy. As far as grain rotations are concerned, OUEA06 is an intermediate case between COEA01 and HNEA01.

To better understand the microscale mechanisms occurring inside the shear band in each specimen, the axes of rotation of the grains in the shear band are analysed: Fig. 10 shows the rotation axes for the rotations in the residual increments for HNEA01 and COEA01. These binned stereoplots are normalised by the *median* value of the number of projected points that enters each bin; the result of this is that bins with a value of 1 (*i.e.*, white in the colour map chosen) represent bins that are at the median value. In both stereoplots, a yellow dot indicates the steepest direction of the shear band projected onto the horizontal plane; note that for both experiments the orientation of the band that develops is neither prescribed nor controlled in the experimental process. In both cases, polarisation of the rotation axis is visible and shows that grains roll preferentially in the steepest direction of the slope. This is particularly striking in COEA01, where rotation axes align very strongly. In HNEA01 it appears that the polarisation is considerably less well-organised in space.

In both cases the rotations are significantly polarised, although not totally so. This is likely due to the complexity of 3D kinematics of rigid particles involved in a deformation mode that has become essentially two-dimensional (a shear band). The polarisation of rotations in Hostun sand are more widely distributed than in COEA01, possibly due to the significantly greater amount of grains involved in the shear band; recall that rotations can be transmitted to neighbouring grains in related, but not strictly identical, orientations.

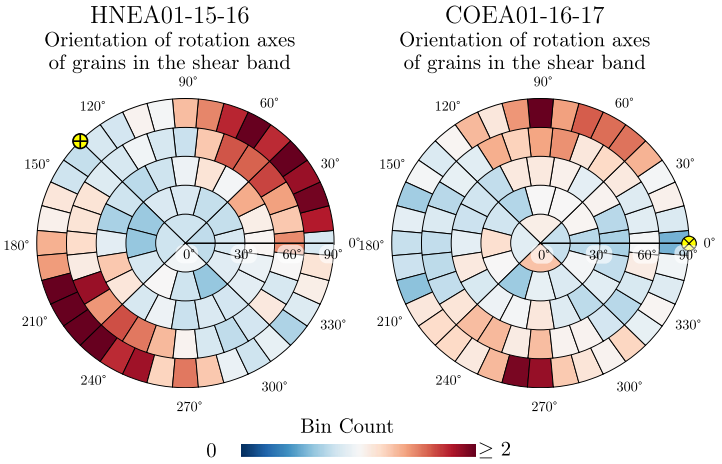

Fig. 10. (Color online.) Comparison of the rotation axes for the grains in the shear band in specimens HNEA01 and COEA01. The yellow dot indicates the orientation of the *direction of maximum slope in the shear band*.

4. Conclusion

In this paper, the emergence of strain localisation in sand has been studied both at the macro- and the microscale, on initially homogeneous, mechanically representative specimens – in the sense of continuum mechanics. The microscale considered is that of the individual sand grains, which is the ultimate one for this material, as long as the grains do not break.

It has been shown that strain localisation manifests itself as a well-defined structure at the specimen scale with strong characteristic properties such as shear band width and orientation with respect to the principal stress directions. The intimate micromechanisms of this localised deformation process have been revealed at the grain scale with x-ray tomography, showing how both the displacement and rotation of individual grains with respect to their neighbours play different and major roles in the kinematics of the shear band: for example the fundamental importance of grain shape in the transmission of individual grain rotations in a mature shear band has been linked to the macroscopic residual stress of the specimen.

The microscale study also brings remarkable observations of early strain localisation events in 3D experiments on sand at a scale between that of the grain and that of the specimen, long before the emergence of the macroscopic shear band, and before the macroscopic stress peak.

It is an open question as to whether these precursors of localisation are linked to the microscale, the specimen scale, the ratio between the two, or whether they can exist simultaneously in a given specimen – or structure – at a range of different scales. Further experimental investigations taking advantage of continuously improving 3D characterisation methods may bring answers to this question by allowing grain-scale analysis of significantly larger specimens in the near future.

Acknowledgements

The laboratory 3SR is part of the LabEx Tec 21 (Investissements d'Avenir – grant agreement No. ANR-11-LABX-0030). The authors also wish to acknowledge the reviewers R.P. Behringer and F. Radjai for their constructive and precious comments which have helped increase the quality of this paper.

References

[1] K.H. Roscoe, The influence of strains in soil mechanics, Geotechnique 20 (2) (1970) 129–170.
[2] I. Vardoulakis, M. Goldscheider, G. Gudehus, Formation of shear bands in sand bodies as a bifurcation problem, Int. J. Numer. Anal. Methods Geomech. 2 (2) (1978) 99–128.
[3] S. Fukushima, F. Tatsuoka, Strength and deformation characteristics of saturated sand at extremely low pressures, Soil Found. 24 (4) (1984) 30–48.
[4] J. Desrues, J. Lanier, P. Stutz, Localization of the deformation in tests on sand sample, Eng. Fract. Mech. 21 (4) (1985) 909–921.
[5] J. Desrues, Naissance des bandes de cisaillement dans les milieux granulaires: expérience et théorie, in: Manuel de rhéologie des geomateriaux, 1985, pp. 279–298.
[6] W. Harris, G. Viggiani, M. Mooney, R. Finno, Use of stereophotogrammetry to analyze the development of shear bands in sand, ASTM Geotech. Test. J. 18 (4) (1995) 405–420.
[7] M. Mokni, J. Desrues, Strain localization measurements in undrained plane-strain biaxial tests on Hostun RF sand, Mech. Cohes.-Frict. Mater. 4 (4) (1999) 419–441.
[8] P. Bésuelle, J. Desrues, S. Raynaud, Experimental characterisation of the localisation phenomenon inside a Vosges sandstone in a triaxial cell, Int. J. Rock Mech. Min. Sci. 37 (8) (2000) 1223–1237.
[9] P. Bésuelle, Compacting and dilating shear bands in porous rock: theoretical and experimental conditions, J. Geophys. Res., Solid Earth 106 (B7) (2001) 13435–13442.

[10] J. Desrues, G. Viggiani, Strain localization in sand: an overview of the experimental results obtained in Grenoble using stereophotogrammetry, Int. J. Numer. Anal. Methods Geomech. 28 (4) (2004) 279–321.
[11] M. Oda, T. Takemura, M. Takahashi, Microstructure in shear band observed by microfocus X-ray computed tomography, Geotechnique 54 (8) (2004) 539–542.
[12] C.A. Coulomb, Essai sur une application des règles de maximis & minimis à quelques problèmes de statique, relatifs à l'architecture, De l'Imprimerie Royale, 1776.
[13] J. Desrues, B. Duthilleul, Mesure du champ de déformation d'un objet plan par la méthode stéréophotogrammétrique de faux relief, J. Méc. Théor. Appl. 3 (1) (1984) 79–103.
[14] J. Torrenti, J. Desrues, E. Benaija, C. Boulay, Stereophotogrammetry and localization in concrete under compression, J. Eng. Mech. 117 (7) (1991) 1455–1465.
[15] J.L. Colliat-Dangus, J. Desrues, P. Foray, Triaxial testing of granular soil under elevated cell pressure, in: ASTM Special Technical Publication, vol. 977, 1988, pp. 290–310.
[16] J. Desrues, R. Chambon, M. Mokni, F. Mazerolle, Void ratio evolution inside shear bands in triaxial sand specimens studied by computed tomography, Geotechnique 46 (3) (1996) 529–546.
[17] J. Desrues, Tracking strain localization in geomaterials using computerized tomography, in: X-Ray CT for Geomaterials, 2004, pp. 15–41.
[18] P. Mollema, M. Antonellini, Compaction bands: a structural analog for anti-mode I cracks in aeolian sandstone, Tectonophysics 267 (1) (1996) 209–228.
[19] P. Besuelle, J.W. Rudnicki, Localization: shear bands and compaction bands, Int. Geophys. 89 (2004) 219–322.
[20] H. Joer, J. Lanier, J. Desrues, E. Flavigny, $1\gamma 2\varepsilon$': a new shear apparatus to study the behavior of granular materials, ASTM Geotech. Test. J. 15 (2) (1992) 129–137.
[21] F. Calvetti, G. Combe, J. Lanier, Experimental micromechanical analysis of a 2D granular material: relation between structure evolution and loading path, Mech. Cohes.-Frict. Mater. 2 (1997) 121–163.
[22] R.P. Behringer, D. Bi, B. Chakraborty, A. Clark, J. Dijksman, J. Ren, J. Zhang, Statistical properties of granular materials near jamming, J. Stat. Mech. Theory Exp. 2014 (6) (2014) P06004, http://stacks.iop.org/1742-5468/2014/i=6/a=P06004.
[23] E. Andò, S.A. Hall, G. Viggiani, J. Desrues, P. Bésuelle, Grain-scale experimental investigation of localised deformation in sand: a discrete particle tracking approach, Acta Geotech. 7 (1) (2012) 1–13.
[24] E. Andò, S.A. Hall, G. Viggiani, J. Desrues, P. Bésuelle, Experimental micromechanics: grain-scale observation of sand deformation, Géotech. Lett. 2 (3) (2012) 107–112.
[25] C. Jaquet, E. Andó, G. Viggiani, H. Talbot, Estimation of separating planes between touching 3D objects using power watershed, in: Mathematical Morphology and Its Applications to Signal and Image Processing, Springer, 2013, pp. 452–463.
[26] P. Bésuelle, P. Lanata, Characterization of the early strain localization in a sandstone and a clay rock, in: 10th International Workshop on Bifurcation and Degradation in Geomaterials, IWBDG 2014, Hong-Kong, May 28–30, 2014, 2014, oral communication.
[27] S.A. Hall, D.M. Wood, E. Ibraim, G. Viggiani, Localised deformation patterning in 2D granular materials revealed by digital image correlation, Granul. Matter 12 (1) (2010) 1–14.
[28] A. Le Bouil, A. Amon, J.-C. Sangleboeuf, H. Orain, P. Bésuelle, G. Viggiani, P. Chasle, J. Crassous, A biaxial apparatus for the study of heterogeneous and intermittent strains in granular materials, Granul. Matter 16 (1) (2014) 1–8, http://dx.doi.org/10.1007/s10035-013-0477-x.
[29] E. Andò, S. Hall, G. Viggiani, J. Desrues, Experimental micro-mechanics of granular media studied by X-ray tomography: recent results and challenges, Géotech. Lett. 3 (2013) 142–146.